Chapter 11

World in a mirror

> Even the butterfly that started the hurricane flapped its wings for a reason.
>
> — Louis Menand, *Thinking Sideways*, New Yorker, 30 March 2015

S O FAR WE HAVE discussed the structure of a group as an abstract entity. Now we switch gears and describe the action of the group on the state space. This is the key step; if a set of solutions is equivalent by symmetry (let's say they live on a circle), we would like to represent it by a single solution (cut the circle at a point, or rewrite the dynamics in a ' symmetry reduced state space', where the circle of equivalent solutions is represented by a single state space point). In this chapter we study quotienting of discrete symmetries, and in chapter 12 we study symmetry reduction for continuous symmetries. We look at individual orbits, and the ways they are interrelated by symmetries. This sets the stage for a discussion of how symmetries affect global densities of trajectories, and the factorization of spectral determinants to be undertaken in chapter 25.

As we shall show here and in chapter 25, discrete symmetries simplify the dynamics in quite a beautiful way: If dynamics is invariant under a set of discrete symmetries G, the state space M is tiled by a set of symmetry-related tiles, and the dynamics can be reduced to dynamics within one such tile, the *fundamental domain* M/G. In presence of a symmetry the notion of a prime periodic orbit has to be reexamined: a set of symmetry-related full state space cycles is replaced by often much shorter *relative periodic orbit*, the shortest segment of the full state space cycle which tiles the cycle and all of its copies under the action of the group. Furthermore, the group operations that relate distinct tiles do double duty as letters of an alphabet which assigns symbolic itineraries to trajectories.

section 14.1

11.1 Symmetries of solutions

Solutions of an equivariant system can satisfy all of system's symmetries, a subgroup of them, or have no symmetry at all. For a generic ergodic orbit $f^t(x)$ the trajectory and any of its images under action of $g \in G$ are distinct with probability one, $f^t(x) \cap gf^{t'}(x) = \emptyset$ for all t, t'. For example, a typical turbulent trajectory of pipe flow has no symmetry beyond the identity, so its symmetry group is the trivial subgroup $\{e\}$. For compact invariant sets, such as fixed points and periodic orbits the situation is very different. For example, the symmetry of the laminar solution of the plane Couette flow is the full symmetry of its Navier-Stokes equations. In between we find solutions whose symmetries are subgroups of the full symmetry of dynamics.

Definition: Isotropy subgroup. The maximal set of group actions which maps a state space point x into itself,

$$G_x = \{g \in G : gx = x\}, \tag{11.1}$$

is called the *isotropy group* (or *stability subgroup* or *little group*) of x. Think of a point $(0, 0, z)$, $z \neq 0$ on z axis in 3 dimensions. Its isotropy group is the O(2) group of rotations in the $\{x, y\}$ plane.

A solution usually exhibits less symmetry than the equations of motion. The symmetry of a solution is thus a subgroup of the symmetry group of dynamics. We thus also need a notion of *set-wise* invariance, as opposed to the above *point-wise* invariance under G_x.

Definition: Symmetry of a solution. We shall refer to the maximal subgroup $G_p \subseteq G$ of actions on state space points within a compact set $\mathcal{M}_p$, which leave no point fixed but leave the set invariant, as the *symmetry G_p* of the solution labelled p,

$$G_p = \{g \in G_p \mid gx \in \mathcal{M}_p, \, gx \neq x \text{ for } g \neq e\}, \tag{11.2}$$

and reserve the notion of 'isotropy' of a set $\mathcal{M}_p$ for the subgroup G_p that leaves each point in it fixed.

A cycle p is G_p-*symmetric* (*set-wise symmetric*, *self-dual*) if the action of elements of G_p on the set of periodic points $\mathcal{M}_p$ reproduces the set. $g \in G_p$ acts as a shift in time, mapping the periodic point $x \in \mathcal{M}_p$ into another periodic point.

Definition: Multiplicity. For a finite discrete group, the multiplicity of orbit p is $m_p = |G|/|G_p|$.

Definition: Stratum.   A stratum is the union of group orbits of the same type: two orbits p, p' belong to the same stratum if and only if their symmetries G_p, $G_{p'}$ are conjugate. In other words, a stratum is to state space what a class is to the set of all group elements in G.

Definition: G_p-fixed orbits: An equilibrium x_q or a compact solution p is point-wise or G_p-*fixed* if it lies in the invariant points subspace $\text{Fix}\left(G_p\right)$, $gx = x$ for all $g \in G_p$, and $x = x_q$ or $x \in \mathcal{M}_p$. A solution that is G-invariant under all group G operations has multiplicity 1. Stability of such solutions will have to be examined with care, as they lie on the boundaries of domains related by the action of the symmetry group.

In the literature the symmetry group of a solution is often called *stabilizer* or *isotropy subgroup*. Saying that G_p is the symmetry of the solution p, or that the orbit $\mathcal{M}_p$ is 'G_p-invariant', accomplishes as much without confusing you with all these names (see remark 10.1). In what follows we say "the symmetry of the periodic orbit p is $Z_2 = \{e, R\}$," rather than bandy about 'stabilizers' and such.

The key concept in the classification of dynamical orbits is their symmetry. We note three types of solutions: (i) fully asymmetric solutions a, (ii) subgroup $G_{\tilde{s}}$ set-wise invariant cycles s built by repeats of relative cycle segments $\tilde{s}$, and (iii) isotropy subgroup G_{EQ}-invariant equilibria or point-wise G_p-fixed cycles b. These are illustrated in figures of examples 11.1 to 11.3.

example 11.2
p. 216

Definition: Asymmetric (or fully asymmetric) orbits.   An orbit (in particular, an equilibrium or periodic orbit) has no symmetry if $\{x_a\} \cap \{gx_a\} = \emptyset$ for any $g \in G$, where $\{x_a\}$ is the set of periodic points belonging to the cycle a. Thus $g \in G$ generate $|G|$ distinct orbits with the same number of points and the same stability properties.

example 11.3
p. 216

example 11.5
p. 217

example 11.6
p. 217

In example 11.7, we illustrate the non-abelian, noncommutative group struc-
ture of the 3-disk game of pinball of sect. 1.3, which has symmetry group elements
that do not commute.

exercise 10.4

example 11.7
p. 218

exercise 11.4
exercise 11.5

Consider next perhaps the simplest 3-dimensional flow with a symmetry, the iconic flow of Lorenz of figure 11.2 (a). The example is long but worth working through: the symmetry-reduced dynamics is much simpler than the original Lorenz flow.

Figure 11.1: The 3-disk pinball cycles: (a) $\overline{12}$, $\overline{13}$, $\overline{23}$, $\overline{123}$; the clockwise $\overline{132}$ not drawn. (b) Cycle $\overline{1232}$; the symmetry related $\overline{1213}$ and $\overline{1323}$ not drawn. (c) Cycle $\overline{12323}$; cycles $\overline{12123}$, $\overline{12132}$, $\overline{12313}$, $\overline{13131}$ and $\overline{13232}$ not drawn. (d) The fundamental domain, i.e., the light-shaded 1/6th wedge in (a), consisting of a section of a disk, two segments of symmetry axes acting as straight mirror walls, and the escape gap to the left. The above 14 full-space cycles restricted to the fundamental domain and recoded in binary reduce to the two fixed points $\overline{0}$, $\overline{1}$, 2-cycle $\overline{10}$, and 5-cycle $\overline{00111}$ (not drawn). See figure 11.3 for the $\overline{001}$ cycle. Work through example 11.6.
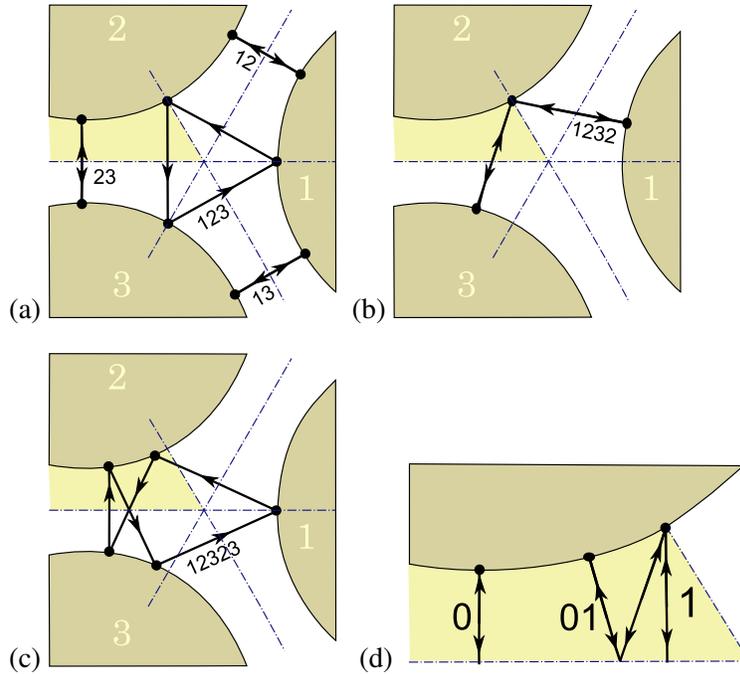
example 11.8
p. 218

example 11.9
p. 219

Note: nonlinear coordinate transformations such as the doubled-polar angle representation (11.13) and figure 11.2 (b) are *not* required to implement the symmetry quotienting $\mathcal{M}/G$. We deploy them only as a visualization aid that might help the reader disentangle 2-dimensional projections of higher-dimensional flows. All numerical calculations can still be carried in the initial, full state space formulation of a flow, with symmetry-related points identified by *linear* symmetry transformations.

in depth:
appendix A25, p. 1206

11.2 Relative periodic orbits

So far we have demonstrated that symmetry relates classes of orbits. Now we show that a symmetry reduces computation of periodic orbits to repeats of shorter, 'relative periodic orbit' segments.

Equivariance of a flow under a symmetry means that the symmetry image of a cycle is again a cycle, with the same period and stability. The new orbit may be topologically distinct (in which case it contributes to the multiplicity of the cycle) or it may be the same cycle.

A cycle p is G_p-*symmetric* under symmetry operation $g \in G_p$ if the operation acts on it as a shift in time, advancing a cycle point to a cycle point on the sym-
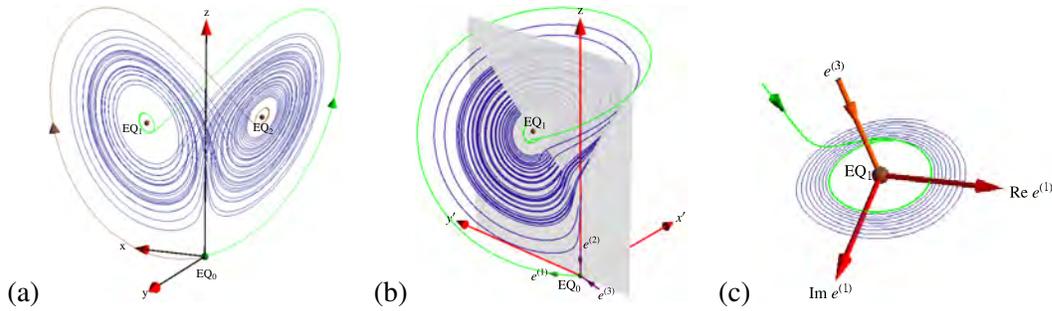
Figure 11.2: (a) Lorenz attractor of figure 3.5, the full state space coordinates $[x, y, z]$, with the unstable manifold orbits $W^u(EQ_0)$. (Green) is a continuation of the unstable $\mathbf{e}^{(1)}$ of EQ_0, and (brown) is its π-rotated symmetric partner. (b) Lorenz attractor plotted in $[\hat{x}, \hat{y}, z]$, the doubled-polar angle coordinates (11.13), with points related by π-rotation in the $[x, y]$ plane identified. Stable eigenvectors of EQ_0: $\mathbf{e}^{(3)}$ and $\mathbf{e}^{(2)}$, along the z axis (11.12). Unstable manifold orbit $W^u(EQ_0)$ (green) is a continuation of the unstable $\mathbf{e}^{(1)}$ of EQ_0. (c) Blow-up of the region near EQ_1: The unstable eigenplane of EQ_1 defined by Re $\mathbf{e}^{(2)}$ and Im $\mathbf{e}^{(2)}$, the stable eigenvector $\mathbf{e}^{(3)}$. The descent of the EQ_0 unstable manifold (green) defines the innermost edge of the strange attractor. As it is clear from (a), it also defines its outermost edge. Work through examples 11.8 and 11.9. (E. Siminos)

metry related segment. The cycle p can thus be subdivided into m_p repeats of a *relative periodic orbit segment*, 'prime' in the sense that the full state space cycle is built from its repeats: see figure 11.1 for examples. Thus, in the presence of a discrete symmetry, the notion of a periodic orbit is replaced by the notion of the shortest segment of the full state space cycle which tiles the cycle under the action of the group. In what follows we refer to this segment as a *relative periodic orbit*. In the literature this is sometimes referred to as a *short periodic orbit*, or, for finite symmetry groups, as a *pre-periodic* orbit.

The relative periodic orbit p (or *its equivariant periodic orbit*) is the orbit $x(t)$ in state space $\mathcal{M}$ which exactly recurs

$$x(t) = g_p \, x(t + T_p) \tag{11.3}$$

for the shortest fixed *relative period* T_p and a fixed group action $g \in G_p$. These group actions are referred to as 'shifts' or, in the case of continuous symmetries, as 'phases.' For a discrete group $g^m = e$ and finite m (10.3), the period of the corresponding full state space orbit is given by the $m_p \times$ (period of the relative periodic orbit), $T_p = |G_p|T_{\tilde{p}}$, and the ith Floquet multiplier $\Lambda_{p,i}$ is given by $\Lambda_{\tilde{p},i}^{m_p}$ of the relative periodic orbit. The elements of the quotient space $b \in G/G_p$ generate the copies bp, so the multiplicity of the full state space cycle p is $m_p = |G|/|G_p|$.

example 11.10
p. 219

11.3 Dynamics reduced to fundamental domain

> I submit my total lack of apprehension of fundamental concepts.
> —John F. Gibson

So far we have used symmetry to effect a reduction in the number of independent cycles, by separating them into classes, and slicing them into 'prime' relative orbit segments. The next step achieves much more: it replaces each class by a single (typically shorter) prime cycle segment.

1. Discrete symmetry tessellates the state space into dynamically equivalent domains, and thus induces a natural partition of state space: If the dynamics is invariant under a discrete symmetry, the state space $\mathcal{M}$ can be completely tiled by a *fundamental domain* $\tilde{\mathcal{M}}$ and its symmetry images $\tilde{\mathcal{M}}_a = a\tilde{\mathcal{M}}$, $\tilde{\mathcal{M}}_b = b\tilde{\mathcal{M}}$, ... under the action of the symmetry group $G = \{e, a, b, \ldots\}$,

$$\mathcal{M} = \tilde{\mathcal{M}} \cup \tilde{\mathcal{M}}_a \cup \tilde{\mathcal{M}}_b \cdots \cup \tilde{\mathcal{M}}_{|G|} . \tag{11.4}$$

See figure 10.1 for an example: the tiling of the 3-disk with 6 copies of the fundamental domain.

2. Discrete symmetry can be used to restrict all computations to the fundamental domain $\tilde{\mathcal{M}} = \mathcal{M}/G$, the reduced state space quotient of the full state space $\mathcal{M}$ by the group actions of G. Several examples are given in figures 11.1, 11.5 and 11.3.

   We can use the invariance condition (10.4) to move the starting point x into the fundamental domain $x = a\tilde{x}$, and then use the relation $a^{-1}b = h^{-1}$ to also relate the endpoint $y \in \tilde{\mathcal{M}}_b$ to its image in the fundamental domain $\tilde{\mathcal{M}}$. While the global trajectory runs over the full space $\mathcal{M}$, the restricted trajectory is brought back into the fundamental domain $\tilde{\mathcal{M}}$ any time it exits into an adjoining tile; the two trajectories are related by the symmetry operation h which maps the global endpoint into its fundamental domain image.

3. Cycle multiplicities induced by the symmetry are removed by reduction of the full dynamics to the dynamics on a fundamental domain. Each symmetry-related set of global cycles p corresponds to precisely one fundamental domain (or relative) cycle $\tilde{p}$.

4. Conversely, each fundamental domain cycle $\tilde{p}$ traces out a segment of the global cycle p, with the end point of the cycle $\tilde{p}$ mapped into the irreducible segment of p with the group element $h_{\tilde{p}}$. A relative periodic orbit segment in the full state space is thus a periodic orbit in the fundamental domain.

5. The group elements $G = \{e, g_2, \ldots, g_{|G|}\}$ which map the fundamental domain $\tilde{\mathcal{M}}$ into its copies $g\tilde{\mathcal{M}}$, serve also as letters of a symbolic dynamics alphabet.

exercise 11.3

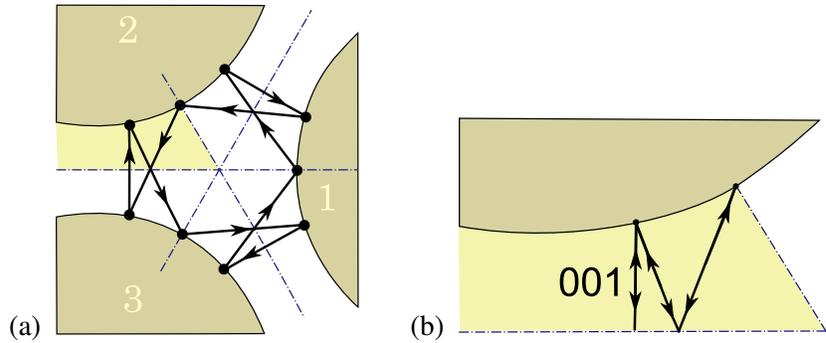For a symmetry reduction in presence of continuous symmetries, see sect. 13.3.

example 11.4
p. 216

example 11.11
p. 219

Figure 11.3: (a) The pair of full-space 9-cycles, the counter-clockwise $\overline{121232313}$ and the clockwise $\overline{131323212}$ correspond to (b) one fundamental domain 3-cycle $\overline{001}$.

(a)   (b)

11.4 Life on the border

In what follows, we shall have to worry also about the boundaries that define the fundamental domain $\tilde{\mathcal{M}}$. Here we by definition include boundaries into the fundamental tile. The state space transformation $g \in G$ leaves invariant the set of *boundary* points (see (11.4))

$$\mathcal{M}_B = \tilde{\mathcal{M}} \cap \tilde{\mathcal{M}}_a \cap \tilde{\mathcal{M}}_b \cdots \cap \tilde{\mathcal{M}}_{|G|} \,. \tag{11.5}$$

Peculiar effects, however, arise for orbits that run along symmetry lines that border a fundamental domain. For example, under reflection σ across a symmetry axis, the axis itself remains invariant. The properties of boundary orbits that belong to G-fixed (point-wise invariant) boundary sets will require a bit of thinking. In our 3-disk example, no such orbits are possible, but they exist in other systems, such as in the bounded region of the Hénon-Heiles potential (remark 11.2), in $1d$ maps of example 11.3, and in Lorenz flow of example 11.8, where the z axis is a G-invariant border. While boundary orbits are invariant under some symmetry operations, their neighborhoods are not.

That's is why one sometimes surgically removes boundaries, and defines

Definition: Free action.   An group action on a state space submanifold $\hat{\mathcal{M}}$ is free if all of the isotropy subgroups G_x, $x \in \hat{\mathcal{M}}$ are trivial.

The fact that open neighborhoods of the border are in part outside of it complicates analysis (linear stability of orbits within the boundary has eigenvectors is the full state space). This affects the Jacobian matrix M_p of the orbit and its Floquet multipliers.

While for low-dimensional state spaces there are typically relatively few boundary orbits, they tend to be among the shortest orbits, and thus play a key role in dynamics.

section 25.4.3

11.5 Invariant polynomials

> All invariants are expressible in terms of a finite number among them. We cannot claim its validity for every group G; rather, it will be our chief task to investigate for each particular group whether a finite integrity basis exists or not; the answer, to be sure, will turn out affirmative in the most important cases.
>
> —Hermann Weyl, a motivational quote on the "so-called first main theorem of invariant theory"

Physical laws should have the same form in symmetry-equivalent coordinate frames, so they are often formulated in terms of functions (Hamiltonians, Lagrangians, $\cdots$) invariant under a given set of symmetries.

Definition: G-invariant function.   A function is said to be G-invariant if

$$f(gx) = f(x) \,, x \in \mathcal{M} \,. \tag{11.6}$$

A G-invariant function is constant along the group orbit of x.

Invariant polynomial functions play a particularly important role in invariant theory. The set of all G-invariant polynomial functions of x which is finitely generated, according to the key result of the representation theory of invariant functions is:

Hilbert-Weyl theorem.   For a compact group G there exists a finite G-invariant homogenous polynomial basis $\{u_1, u_2, \ldots, u_m\}$, $m \geq d$, such that any G-invariant polynomial can be written as a multinomial

$$h(x) = p(u_1(x), u_2(x), \ldots, u_m(x)) \,, \qquad x \in \mathcal{M} \,. \tag{11.7}$$

These polynomials are linearly independent, but can be functionally dependent through nonlinear relations called *syzygies*.

In practice, explicit construction of G-invariant basis can be a laborious undertaking, and we will not take this path except for a few simple low-dimensional cases, such as 'doubled-polar angle representation' (11.13) and the 5-dimensional example of sect. 13.7. We prefer to apply the symmetry to the system as given, rather than undertake a series of nonlinear coordinate transformations that the theorem suggests. (What 'compact' in the above refers to will become clearer after we have discussed continuous symmetries. For now, it suffices to know that any finite discrete group is compact.)

exercise 11.2

example 11.12
p. 220

Résumé

If a dynamical system $(\mathcal{M}, f)$ has a symmetry G, the symmetry should be deployed to 'quotient' the state space to fundamental domain $\hat{\mathcal{M}} = \mathcal{M}/G$, i.e., identify all symmetry-equivalent $x \in \mathcal{M}$ on each group orbit, thus replacing the full state space dynamical system $(\mathcal{M}, f)$ by the symmetry-reduced $(\hat{\mathcal{M}}, \hat{f})$. The main result of this chapter can be stated as follows:

In presence of a discrete symmetry G, associated with each full state space solution p is the group of its symmetries $G_p \subseteq G$ of order $1 \leq |G_p| \leq |G|$, whose elements leave the orbit $\mathcal{M}_p$ invariant. The elements of G_p act on $\mathcal{M}_p$ as shifts, tiling it with $|G_p|$ copies of its shortest invariant segment, the relative periodic orbit $\tilde{p}$. The elements of the coset $b \in G/G_p$ generate $m_p = |G|/|G_p|$ equivalent copies of p.

Once you grasp the relation between the full state space $\mathcal{M}$ and the desymmetrized, G-quotiented reduced state space (fundamental domain) $\mathcal{M}/G$, you will find the life as a fundamentalist so much simpler that you will never return to your full state space ways of yesteryear. The reduction to the fundamental domain $\tilde{\mathcal{M}} = \mathcal{M}/G$ simplifies symbolic dynamics and eliminates symmetry-induced degeneracies. For the short orbits the labor saving is dramatic. For example, for the 3-disk game of pinball there are 256 periodic points of length 8, but reduction to the fundamental domain non-degenerate prime cycles reduces this number to 30. By chapter 24, the savings will be even more dramatic: relative periodic orbits will tile the infinite periodic state space, and replace a numerical simulation of diffusion in the infinite domain by an exact calculation of the diffusion constant, on a compact torus.

Commentary

Remark 11.1. Symmetries of the Lorenz equation.   (Continued from remark 2.3)
After having studied example 11.8 you will appreciate why `ChaosBook.org` starts out
with the symmetry-less Rössler flow (2.28), instead of the better known Lorenz flow
(2.23). Indeed, getting rid of symmetry was one of Rössler's motivations. He threw the
baby out with the water; for Lorenz flow dimensionalities of stable/unstable manifolds
make possible a robust heteroclinic connection absent from Rössler flow, with unstable
manifold of an equilibrium flowing into the stable manifold of another equilibrium. How
such connections are forced upon us is best grasped by perusing the chapter 13 'Hetero-
clinic tangles' of the inimitable Abraham and Shaw Classics Illustrated [1]. Their beau-
tiful hand-drawn sketches elucidate the origin of heteroclinic connections in the Lorenz
flow (and its high-dimensional Navier-Stokes relatives) better than any computer simu-
lation. Miranda and Stone [20] were the first to quotient the Z_2 symmetry and explicitly
construct the desymmetrized, 'proto-Lorenz system', by a nonlinear coordinate transfor-
mation into the Hilbert-Weyl polynomial basis invariant under the action of the symme-
try group [6]. For in-depth discussion of symmetry-reduced ('images') and symmetry-
extended ('covers') topology, symbolic dynamics, periodic orbits, invariant polynomial
bases etc., of Lorenz, Rössler and many other low-dimensional systems there is no better
reference than the Gilmore and Letellier monograph [10]. They interpret [17] the proto-
Lorenz and its 'double cover' Lorenz as 'intensities' being the squares of 'amplitudes',
and call quotiented flows such as (Lorenz)/Z_2 'images.' Our 'doubled-polar angle' visu-
alization of figure 14.15 is a proto-Lorenz in disguise; we, however, integrate the flow and
construct Poincaré sections and return maps in the original Lorenz $[x, y, z]$ coordinates,
without any nonlinear coordinate transformations. The return map figure 14.16 is remi-
niscent in shape both of the one given by Lorenz in his original paper, and the one plotted
in a radial coordinate by Gilmore and Letellier. Nevertheless, it is profoundly different:
our return maps are from unstable manifold $\rightarrow$ itself, and thus intrinsic and coordinate
independent. In this we follow Christiansen *et al.* [5]. This construction is necessary
for high-dimensional flows in order to avoid problems such as double-valuedness of re-
turn map projections on arbitrary 1-dimensional coordinates, encountered already in the
Rössler example of figure 3.4. More importantly, as we know the embedding of the un-
stable manifold into the full state space, a periodic point of our return map *is* - regardless
of the length of the cycle - the periodic point in the full state space, so no additional New-
ton searches are needed. In homage to Lorenz, we note that his return map was already
symmetry-reduced: as z belongs to the symmetry invariant Fix (G) subspace, one can re-
place dynamics in the full space by $\dot{z}, \ddot{z}, \cdots$. That is G-invariant by construction [10].

Remark 11.2. Examples of systems with discrete symmetries.   Almost any flow
of interest is symmetric in some way or other: the list of examples is endless, we list
here a handful that we found interesting. One has a Z_2 symmetry in the Lorenz system
(remark 2.3), the Ising model, and in the 3-dimensional anisotropic Kepler potential [4,
11, 22], a $D_4 = C_{4v}$ symmetry in quartic oscillators [7, 18], in the pure x^2y^2 potential [3,
19] and in hydrogen in a magnetic field [8], and a $D_2 = C_{2v} = V_4 = Z_2 \times Z_2$ symmetry
in the stadium billiard [21]. A number of nontrivial desymmetrizations are carried out in
the Balasz and Voros review [2].   An example of a system with $D_3 = C_{3v}$ symmetry is
provided by the motion of a particle in the Hénon-Heiles potential [12–15], as well as in

the Chernoff-Barrow-Lifshitz-Khalatnikov-,Sinai-Khanin-Shchur cosmology [16].

$$V(r, \theta) = \frac{1}{2}r^2 + \frac{1}{3}r^3 \sin(3\theta) \ .$$

Our 3-disk coding is insufficient for this system because of the existence of elliptic islands and because the three orbits that run along the symmetry axis cannot be labeled in our code. As these orbits run along the boundary of the fundamental domain, they require the special treatment. A partial classification of the 67 possible symmetries of solutions of the plane Couette flow of example 10.9, and their reduction to 5 conjugate classes is given in ref. [9].

References

[1] R. H. Abraham and C. D. Shaw, *Dynamics - The Geometry of Behavior* (Wesley, Reading, MA, 1992).

[2] N. L. Balasz and A. Voros, "Chaos on the pseudosphere", Phys. Rep. **143**, 109–240 (1986).

[3] A. Carnegie and I. C. Percival, "Regular and chaotic motion in some quartic potentials", J. Phys. A **17**, 801 (1984).

[4] F. Christiansen and P. Cvitanović, "Periodic orbit quantization of the anisotropic Kepler problem", Chaos **2**, 61–69 (1992).

[5] F. Christiansen, P. Cvitanović, and V. Putkaradze, "Hopf's last hope: Spatiotemporal chaos in terms of unstable recurrent patterns", Nonlinearity **10**, 55–70 (1997).

[6] D. A. Cox, J. B. Little, and D. 0'Shea, *Ideals, Varieties and Algorithms* (Springer, New York, 2007).

[7] B. Eckhardt, G. Hose, and E. Pollak, "Quantum mechanics of a classically chaotic system: Observations on scars, periodic orbits, and vibrational adiabaticity", Phys. Rev. A **39**, 3776–3793 (1989).

[8] B. Eckhardt and D. Wintgen, "Symbolic description of periodic orbits for the quadratic Zeeman effect", J. Phys. B **23**, 355–363 (1990).

[9] J. F. Gibson, J. Halcrow, and P. Cvitanović, "Equilibrium and traveling-wave solutions of plane Couette flow", J. Fluid Mech. **638**, 243–266 (2009).

[10] R. Gilmore and C. Letellier, *The Symmetry of Chaos* (Oxford Univ. Press, Oxford, 2007).

[11] M. C. Gutzwiller, "The quantization of a classically ergodic system", Physica D **5**, 183–207 (1982).

[12] M. Hénon and C. Heiles, "The applicability of the third integral of motion: Some numerical experiments", Astron. J. **69**, 73–79 (1964).

[13] C. Jung and P. Richter, "Classical chaotic scattering-periodic orbits, symmetries, multifractal invariant sets", J. Phys. A **23**, 2847 (1990).

[14] C. Jung and H. J. Scholz, "Cantor set structures in the singularities of classical potential scattering", J. Phys. A **20**, 3607 (1987).

[15] B. Lauritzen, "Discrete symmetries and the periodic-orbit expansions", Phys. Rev. A **43**, 603–606 (1991).

[16] O. M. Lecian, "Reflections on the hyperbolic plane", Int. J. Mod. Phys. D **22**, 1350085 (2013).

[17] C. Letellier and R. Gilmore, "Covering dynamical systems: Two-fold covers", Phys. Rev. E **63**, 016206 (2001).

[18] C. C. Martens, R. L. Waterland, and W. P. Reinhardt, "Classical, semiclassical, and quantum mechanics of a globally chaotic system: Integrability in the adiabatic approximation", J. Chem. Phys. **90**, 2328 (1989).

[19] S. G. Matanyan, G. K. Savvidy, and N. G. Ter-Arutyunyan-Savvidy, "Classical Yang-Mills mechanics. Nonlinear colour oscillations", Sov. Phys. JETP **80**, 830–838 (1981).

[20] R. Miranda and E. Stone, "The proto-Lorenz system", Phys. Lett. A **178**, 105–113 (1993).

[21] J. M. Robbins, "Discrete symmetries in periodic-orbit theory", Phys. Rev. A **40**, 2128–2136 (1989).

[22] G. Tanner and D. Wintgen, "Quantization of chaotic systems", Chaos **2**, 53 (1992).
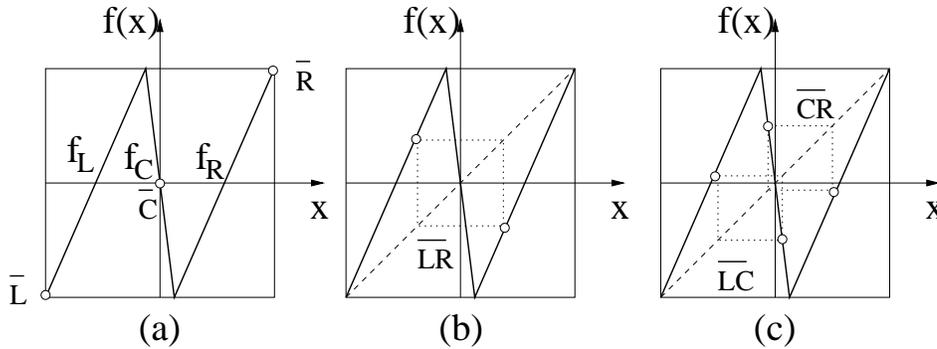
Figure 11.4: The D_1-equivariant bimodal sawtooth map of figure 10.2 has three types of periodic orbits: (a) D_1-fixed fixed point $\overline{C}$, asymmetric fixed points pair $\{\overline{L},\overline{R}\}$. (b) D_1-symmetric (setwise invariant) 2-cycle $\overline{LR}$, composed of the relative cycle segment from L to R and its repeat from R to L. (c) Asymmetric 2-cycles pair $\{\overline{LC},\overline{CR}\}$. (study example 11.3; continued in figure 11.5) (Y. Lan)

11.6 Examples

Example 11.1. D_1-symmetric cycles. For D_1 the period of a set-wise symmetric cycle is even ($n_s = 2n_{\tilde{s}}$), and the mirror image of the x_s periodic point is reached by traversing the relative periodic orbit segment $\tilde{s}$ of length $n_{\tilde{s}}$, $f^{n_{\tilde{s}}}(x_s) = \sigma x_s$, see figure 11.4 (b).

Example 11.2. D_1-invariant cycles. In the example at hand there is only one G-invariant (point-wise invariant) orbit, the fixed point $\overline{C}$ at the origin, see figure 11.4 (a). As reflection symmetry is the only discrete symmetry that a map of the interval can have, this example completes the group-theoretic analysis of 1-dimensional maps. We shall continue analysis of this system in example 11.4, and work out the symbolic dynamics of such reflection symmetric systems in example 15.6.

Example 11.3. Group D_1 - a reflection symmetric $1d$ map. Consider the bimodal 'sawtooth' map of figure 11.4, with the state space $\mathcal{M} = [-1, 1]$ split into three regions $\mathcal{M} = \{\mathcal{M}_L, \mathcal{M}_C, \mathcal{M}_R\}$ which we label with a 3-letter alphabet L(eft), C(enter), and R(ight). The symbolic dynamics is complete ternary dynamics, with any sequence of letters $\mathcal{A} = \{L, C, R\}$ corresponding to an admissible trajectory ('complete' means no additional grammar rules required, see example 14.7 below). The D_1-equivariance of the map, $D_1 = \{e, \sigma\}$, implies that if $\{x_n\}$ is a trajectory, so is $\{\sigma x_n\}$.

Fix (G), the set of points invariant under group action of D_1, $\tilde{\mathcal{M}} \cap \sigma\tilde{\mathcal{M}}$, is just this fixed point $x = 0$, the reflection symmetry point. If a is an asymmetric cycle, σ maps it into the reflected cycle σa, with the same period and the same stability properties, see the fixed points pair $\{\overline{L}, \overline{R}\}$ and the 2-cycles pair $\{\overline{LC}, \overline{CR}\}$ in figure 11.4 (c).

Example 11.4. Group D_1 and reduction to the fundamental domain. Consider again the reflection-symmetric bimodal Ulam sawtooth map $f(-x) = -f(x)$ of example 11.3, with symmetry group $D_1 = \{e, \sigma\}$. The state space $\mathcal{M} = [-1, 1]$ can be tiled by half-line $\tilde{\mathcal{M}} = [0, 1]$, and $\sigma\tilde{\mathcal{M}} = [-1, 0]$, its image under a reflection across $x = 0$ point. The

Figure 11.5: The bimodal Ulam sawtooth map of figure 11.4 with the D_1 symmetry $f(-x) = -f(x)$, restricted to the fundamental domain. $f(x)$ is indicated by the thin line, and fundamental domain map $\tilde{f}(\tilde{x})$ by the thick line. (a) Boundary fixed point $\overline{C}$ is the fixed point $\overline{0}$. The asymmetric fixed point pair $\{\overline{L},\overline{R}\}$ is reduced to the fixed point $\overline{2}$, and the full state space symmetric 2-cycle $\overline{LR}$ is reduced to the fixed point $\overline{1}$. (b) The asymmetric 2-cycle pair $\{\overline{LC},\overline{CR}\}$ is reduced to 2-cycle $\overline{01}$. (c) All fundamental domain fixed points and 2-cycles. (work through example 11.4)   (Y. Lan)
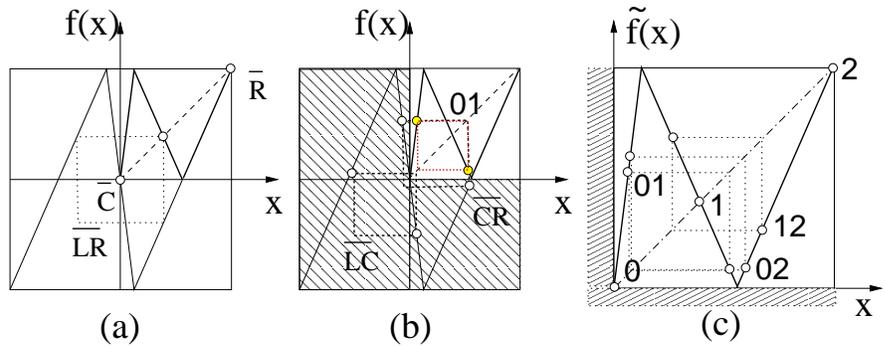
dynamics can then be restricted to the *fundamental domain* $\tilde{x}_k \in \tilde{\mathcal{M}} = [0, 1]$; every time a trajectory leaves this interval, it is mapped back using σ.

In figure 11.5 the fundamental domain map $\tilde{f}(\tilde{x})$ is obtained by reflecting $x < 0$ segments of the global map $f(x)$ into the upper right quadrant. $\tilde{f}$ is also bimodal and piecewise-linear, with $\tilde{\mathcal{M}} = [0, 1]$ split into three regions $\tilde{\mathcal{M}} = \{\tilde{\mathcal{M}}_0, \tilde{\mathcal{M}}_1, \tilde{\mathcal{M}}_2\}$ which we label with a 3-letter alphabet $\tilde{\mathcal{A}} = \{0, 1, 2\}$. The symbolic dynamics is again complete ternary dynamics, with any sequence of letters $\{0, 1, 2\}$ admissible.

However, the interpretation of the 'desymmetrized' dynamics is quite different - the multiplicity of every periodic orbit is now 1, and relative periodic segments of the full state space dynamics are all periodic orbits in the fundamental domain. Consider figure 11.5:

In (a) the boundary fixed point $\overline{C}$ is also the fixed point $\overline{0}$. The asymmetric fixed point pair $\{\overline{L},\overline{R}\}$ is reduced to the fixed point $\overline{2}$, and the full state space symmetric 2-cycle $\overline{LR}$ is reduced to the fixed point $\overline{1}$. (b) The asymmetric 2-cycle pair $\{\overline{LC},\overline{CR}\}$ is reduced to the 2-cycle $\overline{01}$. Finally, the symmetric 4-cycle $\overline{LCRC}$ is reduced to the 2-cycle $\overline{02}$. This completes the conversion from the full state space for all fundamental domain fixed points and 2-cycles, frame (c).

Example 11.5. $C_{3v} = D_3$ symmetry of the 3-disk game of pinball.   If the three unit-radius disks in figure 10.1 are equidistantly spaced, our game of pinball has a sixfold symmetry. The symmetry group of relabeling the 3 disks is the permutation group S_3; however, it is more instructive to think of this group geometrically, as C_{3v}, also known as the dihedral group

$$D_3 = \{e, \sigma_{12}, \sigma_{13}, \sigma_{23}, C^{1/3}, C^{2/3}\}, \tag{11.8}$$

the group of order $|G| = 6$ consisting of the identity element e, three reflections across symmetry axes $\{\sigma_{12}, \sigma_{23}, \sigma_{13}\}$, and two rotations by $2\pi/3$ and $4\pi/3$ denoted $\{C^{1/3}, C^{2/3}\}$. (continued in example 11.6)

Example 11.6. 3-disk game of pinball - symmetry-related orbits.   (Continued from example 11.5)   Applying an element (identity, rotation by $\pm 2\pi/3$, or one of the three possible reflections) of this symmetry group to a trajectory yields another trajectory. For instance, σ_{23}, the flip across the symmetry axis going through disk 1 interchanges the symbols 2 and 3; it maps the cycle $\overline{12123}$ into $\overline{13132}$, figure 11.1 (c). Cycles $\overline{12}$, $\overline{23}$, and $\overline{13}$ in figure 11.1 (a) are related to each other by rotation by $\pm 2\pi/3$, or, equivalently, by a relabeling of the disks. (continued in example 10.7)

Figure 11.6: Cycle $\overline{121212313}$ has multiplicity 6; shown here is $\overline{121313132} = \sigma_{23}\overline{121212313}$. However, $\overline{121231313}$ which has the same stability and period is related to $\overline{121313132}$ by time reversal, but not by any C_{3v} symmetry.
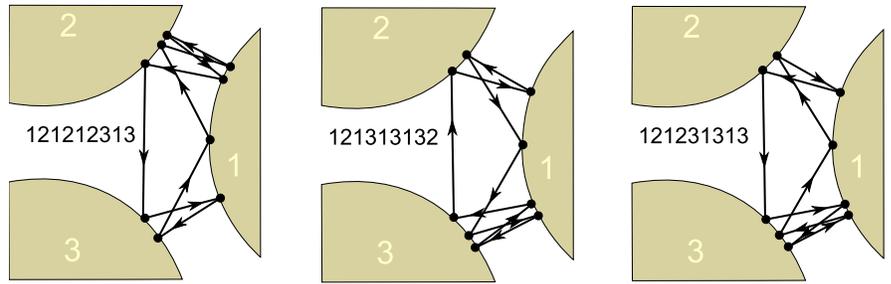
Example 11.7. 3-disk game of pinball - cycle symmetries. (Continued from example 10.8) The C_3 subgroup $G_p = \{e, C^{1/3}, C^{2/3}\}$ invariance is exemplified by the two cycles $\overline{123}$ and $\overline{132}$ which are invariant under rotations by $2\pi/3$ and $4\pi/3$, but are mapped into each other by any reflection, figure 11.6 (a), and have multiplicity $|G|/|G_p| = 2$.

The C_v type of a subgroup is exemplified by the symmetries of $\hat{p} = 1213$. This cycle is invariant under reflection $\sigma_{23}\{\overline{1213}\} = \overline{1312} = \overline{1213}$, so the invariant subgroup is $G_{\hat{p}} = \{e, \sigma_{23}\}$, with multiplicity is $m_{\hat{p}} = |G|/|G_p| = 3$; the cycles in this class, $\overline{1213}, \overline{1232}$ and $\overline{1323}$, are related by $2\pi/3$ rotations, figure 11.6 (b).

A cycle of no symmetry, such as $\overline{12323}$, has $G_p = \{e\}$ and contributes in all six copies (the remaining cycles in the class are $\overline{12132}, \overline{12313}, \overline{12323}, \overline{13132}$ and $\overline{13232}$), figure 11.6 (c).

Besides the above spatial symmetries, for Hamiltonian systems cycles may be related by time reversal symmetry. An example are the cycles $\overline{121212313}$ and $\overline{313212121} = \overline{121213132}$ which have the same periods and stabilities, but are related by no space symmetry, see figure 11.6. (continued in example 11.11)

Example 11.8. Desymmetrization of Lorenz flow. (Continuation of example 10.6) Lorenz equation (10.14) is equivariant under (10.15), the action of order-2 group $Z_2 = \{e, C^{1/2}\}$, where $C^{1/2}$ is $[x, y]$-plane, half-cycle rotation by π about the z-axis:

$$(x, y, z) \to C^{1/2}(x, y, z) = (-x, -y, z). \tag{11.9}$$

$(C^{1/2})^2 = 1$ condition decomposes the state space into two linearly irreducible subspaces $\mathcal{M} = \mathcal{M}^+ \oplus \mathcal{M}^-$, the z-axis $\mathcal{M}^+$ and the $[x, y]$ plane $\mathcal{M}^-$, with projection operators onto the two subspaces given by

$$\mathbf{P}^+ = \frac{1}{2}(1 + C^{1/2}) = \begin{pmatrix} 0 & 0 & 0 \\ 0 & 0 & 0 \\ 0 & 0 & 1 \end{pmatrix}, \quad \mathbf{P}^- = \frac{1}{2}(1 - C^{1/2}) = \begin{pmatrix} 1 & 0 & 0 \\ 0 & 1 & 0 \\ 0 & 0 & 0 \end{pmatrix}. \tag{11.10}$$

As the flow is Z_2-invariant, so is its linearization $\dot{x} = Ax$. Evaluated at EQ_0, A commutes with $C^{1/2}$, and, as we have already seen in example 4.6, the EQ_0 stability matrix decomposes into $[x, y]$ and z blocks.

The 1-dimensional $\mathcal{M}^+$ subspace is the fixed-point subspace, with the z-axis points left *point-wise invariant* under the group action

$$\mathcal{M}^+ = \text{Fix}(Z_2) = \{x \in \mathcal{M} \mid g\, x = x \text{ for } g \in \{e, C^{1/2}\}\} \tag{11.11}$$

(here $x = (x, y, z)$ is a 3-dimensional vector, not the coordinate x). A Z_2-fixed point $x(t)$ in Fix(Z_2) moves with time, but according to (10.10) remains within $x(t) \in \text{Fix}(Z_2)$ for all

times; the subspace $\mathcal{M}^+ = \text{Fix}(Z_2)$ is *flow invariant*. In case at hand this jargon is a bit of an overkill: clearly for $(x, y, z) = (0, 0, z)$ the full state space Lorenz equation (10.14) is reduced to the exponential contraction to the EQ_0 equilibrium,

$$\dot{z} = -b\,z\,. \tag{11.12}$$

However, for higher-dimensional flows the flow-invariant subspaces can be high-dimensional, with interesting dynamics of their own. Even in this simple case this subspace plays an important role as a topological obstruction: the orbits can neither enter it nor exit it, so the number of windings of a trajectory around it provides a natural, topological symbolic dynamics.

The $\mathcal{M}^-$ subspace is, however, *not* flow-invariant, as the nonlinear terms $\dot{z} = xy - bz$ in the Lorenz equation (10.14) send all initial conditions within $\mathcal{M}^- = (x(0), y(0), 0)$ into the full, $z(t) \neq 0$ state space $\mathcal{M}/\mathcal{M}^+$. (continued in example 11.9)

(E. Siminos and J. Halcrow)

Example 11.9. Lorenz flow in doubled-polar angle representation. By taking as a Poincaré section any $C^{1/2}$-equivariant, non-self-intersecting surface that contains the z axis, the state space is divided into a half-space fundamental domain $\tilde{\mathcal{M}} = \mathcal{M}/Z_2$ and its 180° rotation $C^{1/2}\tilde{\mathcal{M}}$. An example is afforded by the $\mathcal{P}$ plane section of the Lorenz flow in figure 3.5. Take the fundamental domain $\tilde{\mathcal{M}}$ to be the half-space between the viewer and $\mathcal{P}$. Then the full Lorenz flow is captured by re-injecting back into $\tilde{\mathcal{M}}$ any trajectory that exits it, by a rotation of π around the z axis.

As any such $C^{1/2}$-invariant section does the job, a choice of a 'fundamental domain' is here largely mater of taste. For purposes of visualization it is convenient to make the double-cover nature of the full state space by $\tilde{\mathcal{M}}$ explicit, through any state space redefinition that maps a pair of points related by symmetry into a single point. In case at hand, this can be easily accomplished by expressing (x, y) in polar coordinates $(x, y) = (r\cos\theta, r\sin\theta)$, and then plotting the flow in the *'doubled-polar angle representation:'*

$$(\hat{x}, \hat{y}, z) = (r\cos 2\theta, r\sin 2\theta, z) = ((x^2 - y^2)/r, 2xy/r, z)\,, \tag{11.13}$$

as in figure 11.2 (b). In contrast to the original G-equivariant coordinates $[x, y, z]$, the Lorenz flow expressed in the new coordinates $[\hat{x}, \hat{y}, z]$ is G-*invariant*, see example 11.12. In this representation the $\tilde{\mathcal{M}} = \mathcal{M}/Z_2$ fundamental domain flow is a smooth, continuous flow, with (any choice of) the fundamental domain stretched out to seamlessly cover the entire $[\hat{x}, \hat{y}]$ plane. (continued in example 14.4)

(E. Siminos and J. Halcrow)

Example 11.10. Relative periodic orbits of Lorenz flow. (Continuation of example 11.8) The relation between the full state space periodic orbits, and the fundamental domain (11.13) reduced relative periodic orbits of the Lorenz flow: an asymmetric full state space cycle pair p, Rp maps into a single cycle $\tilde{p}$ in the fundamental domain, and any self-dual cycle $p = Rp = \tilde{p}R\tilde{p}$ is a repeat of a relative periodic orbit $\tilde{p}$.

Example 11.11. 3-disk game of pinball in the fundamental domain.

If the dynamics is equivariant under interchanges of disks, the absolute disk labels $\epsilon_i = 1, 2, \cdots, N$ can be replaced by the symmetry-invariant relative disk→disk increments g_i, where g_i is the discrete group element that maps disk $i-1$ into disk i. For 3-disk system

g_i is either reflection σ back to initial disk (symbol '0') or $2\pi/3$ rotation by C to the next disk (symbol '1'). An immediate gain arising from symmetry invariant relabeling is that N-disk symbolic dynamics becomes $(N-1)$-nary, with no restrictions on the admissible sequences.

An irreducible segment corresponds to a periodic orbit in the *fundamental domain*, a one-sixth slice of the full 3-disk system, with the symmetry axes acting as reflecting mirrors (see figure 11.1(d)). A set of orbits related in the full space by discrete symmetries maps onto a single fundamental domain orbit. The reduction to the fundamental domain desymmetrizes the dynamics and removes all global discrete symmetry-induced degeneracies: rotationally symmetric global orbits (such as the 3-cycles $\overline{123}$ and $\overline{132}$) have multiplicity 2, reflection symmetric ones (such as the 2-cycles $\overline{12}$, $\overline{13}$ and $\overline{23}$) have multiplicity 3, and global orbits with no symmetry are 6-fold degenerate. Table 15.2 lists some of the shortest binary symbols strings, together with the corresponding full 3-disk symbol sequences and orbit symmetries. Some examples of such orbits are shown in figures 11.6 and 11.3. (continued in example 15.7)

Example 11.12. Polynomials invariant under discrete operations on $\mathbb{R}^3$. (Continued from example 10.3) σ is a *reflection* through the $[x,y]$ plane. Any $\{e,\sigma\}$-invariant function can be expressed in the polynomial basis $\{u_1, u_2, u_3\} = \{x, y, z^2\}$.

$C^{1/2}$ is a $[x,y]$-plane *rotation* by π about the z-axis. Any $\{e, C^{1/2}\}$-invariant function can be expressed in the polynomial basis $\{u_1, u_2, u_3, u_4\} = \{x^2, xy, y^2, z\}$, with one syzygy between the basis polynomials, $(x^2)(y^2) - (xy)^2 = 0$.

P is an *inversion* through the point $(0, 0, 0)$. Any $\{e, P\}$-invariant function can be expressed in the polynomial basis $\{u_1, \cdots, u_6\} = \{x^2, y^2, z^2, xy, xz, yz\}$, with three syzygies between the basis polynomials, $(x^2)(y^2) - (xy)^2 = 0$, and its 2 permutations.

For the D_2 dihedral group $G = \{e, \sigma, C^{1/2}, P\}$ the G-invariant polynomial basis is $\{u_1, u_2, u_3, u_4\} = \{x^2, y^2, z^2, xy\}$, with one syzygy, $(x^2)(y^2) - (xy)^2 = 0$.

Exercises

11.1. $G_x \subset G$. The maximal set of group actions which maps a state space point x into itself,

$$G_x = \{g \in G : gx = x\}, \qquad (11.14)$$

is called the *isotropy group* (or *stability subgroup* or *little group*) of x. Prove that the set G_x as defined in (11.14) is a subgroup of G.

11.2. **Polynomials invariant under discrete operations on** $\mathbb{R}^3$. Prove that the $\{e, \sigma\}$, $\{e, C^{1/2}\}$, $\{e, P\}$ and $\{e, \sigma, C^{1/2}, P\}$-invariant polynomial basis and syzygies are those listed in example 11.12.

11.3. **Reduction of 3-disk symbolic dynamics to binary.** (continued from exercise 1.1)

   (a) Verify that the 3-disk cycles
   $\{\overline{1\,2}, \overline{1\,3}, \overline{2\,3}\}$, $\{\overline{1\,2\,3}, \overline{1\,3\,2}\}$, $\{\overline{12\,13} + 2 \text{ perms.}\}$,
   $\{\overline{121\,232\,313} + 5 \text{ perms.}\}$, $\{\overline{121\,323} + 2 \text{ perms.}\}$,
   $\cdots$,
   correspond to the fundamental domain cycles $\overline{0}$, $\overline{1}$, $\overline{01}$, $\overline{001}$, $\overline{011}$, $\cdots$ respectively.

   (b) Check the reduction for short cycles in table 15.2 by drawing them both in the full 3-disk system and in the fundamental domain, as in figure 11.3.

   (c) Optional: Can you see how the group elements listed in table 15.2 relate irreducible segments to the fundamental domain periodic orbits?

   (continued in exercise 15.7)

11.4. **Lorenz system in polar coordinates: group theory.** Use (A2.13), (A2.14) to rewrite the Lorenz equation (10.18) in polar coordinates (r, θ, z), where $(x, y) = (r \cos \theta, r \sin \theta)$.

   1. Show that in the polar coordinates Lorenz flow takes form

   $$\begin{aligned} \dot{r} &= \frac{r}{2}(-\sigma - 1 + (\sigma + \rho - z)\sin 2\theta \\ &\quad + (1 - \sigma)\cos 2\theta) \\ \dot{\theta} &= \frac{1}{2}(-\sigma + \rho - z + (\sigma - 1)\sin 2\theta \\ &\quad + (\sigma + \rho - z)\cos 2\theta) \\ \dot{z} &= -bz + \frac{r^2}{2}\sin 2\theta. \end{aligned} \qquad (11.15)$$

   2. Argue that the transformation to polar coordinates is invertible almost everywhere. Where does the inverse not exist? What is group-theoretically special about the subspace on which the inverse not exist?

3. Show that this is the (Lorenz)/Z_2 quotient map for the Lorenz flow, i.e., that it identifies points related by the π rotation in the $[x, y]$ plane.

4. Rewrite (10.18) in the invariant polynomial basis of example 11.12 and exercise 11.15.

5. Show that a periodic orbit of the Lorenz flow in polar representation (11.15) is either a periodic orbit or a relative periodic orbit (11.3) of the Lorenz flow in the (x, y, z) representation.

By going to polar coordinates we have quotiented out the π-rotation $(x, y, z) \to (-x, -y, z)$ symmetry of the Lorenz equations, and constructed an explicit representation of the desymmetrized Lorenz flow.

11.5. **Proto-Lorenz system.** Here we quotient out the Z_2 symmetry by constructing an explicit "intensity" representation of the desymmetrized Lorenz flow, following Miranda and Stone [20].

   1. Rewrite the Lorenz equation (10.14) in terms of variables

   $$(u, v, z) = (x^2 - y^2, 2xy, z), \qquad (11.16)$$

   show that it takes form

   $$\begin{bmatrix} \dot{u} \\ \dot{v} \\ \dot{z} \end{bmatrix} = \begin{bmatrix} -(\sigma + 1)u + (\sigma - r)v + (1 - \sigma)N + vz \\ (r - \sigma)u - (\sigma + 1)v + (r + \sigma)N - uz - uN \\ v/2 - bz \end{bmatrix}$$
   $$N = \sqrt{u^2 + v^2}. \qquad (11.17)$$

   2. Show that this is the (Lorenz)/Z_2 quotient map for the Lorenz flow, i.e., that it identifies points related by the π rotation (11.9).

   3. Show that (11.16) is invertible. Where does the inverse not exist?

   4. Compute the equilibria of proto-Lorenz and their stabilities. Compare with the equilibria of the Lorenz flow.

   5. Plot the strange attractor both in the original form (10.14) and in the proto-Lorenz form (11.17)
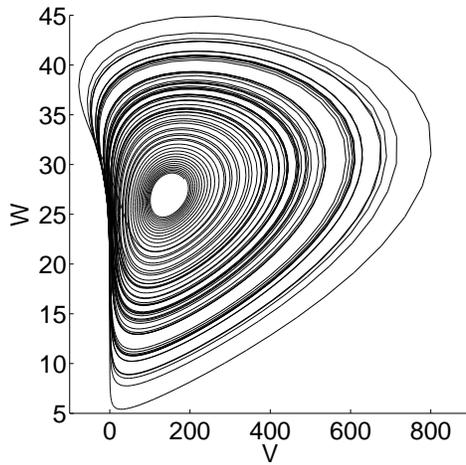
for the Lorenz parameter values $\sigma = 10$, $b = 8/3$, $\rho = 28$. Topologically, does it resemble more the Lorenz, or the Rössler attractor, or neither? (plot by J. Halcrow)

7. Show that a periodic orbit of the proto-Lorenz is either a periodic orbit or a relative periodic orbit of the Lorenz flow.

8. Show that if a periodic orbit of the proto-Lorenz is also periodic orbit of the Lorenz flow, their Floquet multipliers are the same. How do the Floquet multipliers of relative periodic orbits of the Lorenz flow relate to the Floquet multipliers of the proto-Lorenz?

9 What does the volume contraction formula (4.42) look like now? Interpret.

10. Show that the coordinate change (11.16) is the same as rewriting (11.15) in variables

$$(u, v) = (r^2 \cos 2\theta, r^2 \sin 2\theta),$$

i.e., squaring a complex number $z = x + iy$, $z^2 = u + iv$.

11. How is (11.17) related to the invariant polynomial basis of example 11.12 and exercise 11.15?